Manipulating Association of Electroactive Chromophores via the Use of Peptidic Templates

Onur Y. Kas,[†] Manoj B. Charati,[†] Kristi L. Kiick,*[,†] and Mary E. Galvin*[,‡]

Department of Materials Science and Engineering, University of Delaware, Newark, Delaware 19716, and Air Products and Chemicals, Allentown, Pennsylvania 18195

Received December 28, 2005. Revised Manuscript Received April 27, 2006

The performance of organic or polymeric devices such as light-emitting diodes, thin-film transistors, and photovoltaic devices depends on the alignment and spacing between electroactive chains, but achieving such control on angstrom length scales has proven a significant challenge. It is well-known that Nature executes such accurate regulation at a molecular level in proteins and that polypeptidic scaffolds can be used to organize functional groups. We have therefore employed peptidic scaffolds to align multiple electroactive molecules in desired orientations and spacing to manipulate the electronic behavior of side chains. The controlled electronic behavior of the hybrid molecules with small changes in architecture was indicated via photoluminescence, photoluminescence excitation, and ^{1}H NMR spectroscopy. Methylstilbene molecules form a ground-state complex and excimer when placed approximately 6 Å apart on the same side of a peptide chain, but act independently when placed on opposite sides of the chain or at longer distances. These results prove that peptidic scaffolds can be used to control interactions and photophysics in electroactive organics, at distances relevant for electroactive devices.

Introduction

Although substantial progress has been made, over the last 15 years, in grasping the fundamental rules that govern the behavior of semiconducting materials, control of the intrinsic properties of these materials via manipulation of intermolecular spacing and spatial orientation/conformation has remained elusive.[1−4] Intermolecular communication plays a critical role in determining the structure/property relationships of electroactive organic molecules and critically impacts the performance of most organic semiconductor devices such as light-emitting diodes (LEDs), field-effect transistors (FETs), and photovoltaic (PV) devices. For instance, in organic light-emitting diodes or polymeric light-emitting diodes (OLEDs or PLEDs), the device efficiency depends on both the carrier mobility and photoluminescence (PL) yield, with mobility decreasing and photoluminescence increasing as the intermolecular distance increases.[4−6] In PV devices stacking between molecules and $\pi-\pi$ overlap can significantly increase carrier mobility. Exciton splitting, a critical step to obtaining high efficiency in PV devices, is dependent on the distance between hole- and electron-transporting groups,[7−9] with the requirement that hole- and electron-transporting groups must be closer than the exciton diffusion length. Similarly, in organic FET devices, it has been shown that $\pi-\pi$ interactions significantly increase mobility.[5,10]

As these design principles have been known for years, a variety of templates have been explored to control and study length scales over which photophysical and transport properties vary. Of previously employed strategies, template-based molecular assembly has been used to study the effect of certain conformational parameters and spatial arrangement on device performance. For example, U-shaped templates such as 1,8-naphthalene[11] and 1,8-anthracene[12] have been employed to confine chromophores and probe intermolecular interactions. The use of *N*,*N*′-diarylurea-based templates,[13] paracyclophane templates,[14] or Langmuir−Blodgett films[15−17] has also been reported. Although these systems have been able to mimic aggregation-like behavior successfully, they

[†] University of Delaware.
[‡] Air Products and Chemicals.

(1) Sirringhaus, H.; Brown, P. J.; Friend, R. H.; Nielsen, M. M.; Bechgaard, K.; Langeveld-Voss, B. M. W.; Spiering, A. J. H.; Janssen, R. A. J.; Meijer, E. W.; Herwig, P.; De Leeuw, D. M. *Nature (London)* **1999**, *401*, (6754), 685−688.
(2) Gettinger, C. L.; Heeger, A. J.; Drake, J. M.; Pine, D. J. *J. Chem. Phys.* **1994**, *101* (2), 1673−8.
(3) Lucht, B. L.; Mao, S. S. H.; Tilley, T. D. *J. Am. Chem. Soc.* **1998**, *120* (18), 4354−4365.
(4) Nguyen, T. Q.; Martini, I. B.; Liu, J.; Schwartz, B. J. *J. Phys. Chem. B* **2000**, *104* (2), 237−255.
(5) Sirringhaus, H.; Brown, P. J.; Friend, R. H.; Nielsen, M. M.; Bechgaard, K.; Langeveld-Voss, B. M. W.; Spiering, A. J. H.; Janssen, R. A. J.; Meijer, E. W. *Synth. Met.* **2000**, *111*, 129−132.
(6) Jakubiak, R.; Bao, Z.; Rothberg, L. *Synth. Met.* **2000**, *114* (1), 61−64.
(7) Spanggaard, H.; Krebs, F. C. *Sol. Energy Mater. Sol. Cells* **2004**, *83* (2−3), 125−146.
(8) Peumans, P.; Yakimov, A.; Forrest, S. R. *J. Appl. Phys.* **2003**, *93* (7), 3693−3723.
(9) Shaheen, S. E.; Brabec, C. J.; Sariciftci, N. S.; Padinger, F.; Fromherz, T.; Hummelen, J. C. *Appl. Phy. Lett.* **2001**, *78* (6), 841−843.
(10) Laquindanum, J. G.; Katz, H. E.; Lovinger, A. J.; Dodabalapur, A. *Chem. Mater.* **1996**, *8* (11), 2542.
(11) Iyoda, M.; Kondo, T.; Nakao, K.; Hara, K.; Kuwatani, Y.; Yoshida, M.; Matsuyama, H. *Org. Lett.* **2000**, *2* (14), 2081−2083.
(12) Crisp, G. T.; Turner, P. D. *Tetrahedron* **2000**, *56* (42), 8335−8344.
(13) Ricks, H. L.; Shimizu, L. S.; Smith, M. D.; Bunz, U. H. F.; Shimizu, K. D. *Tetrahedron Lett.* **2004**, *45* (16), 3229−3232.
(14) Bartholomew, G. P.; Bazan, G. C. *Acc. Chem. Res.* **2001**, *34* (1), 30−39.
(15) Whitten, D. G. *Acc. Chem. Res.* **1993**, *26* (9), 502−509.
(16) Krebs, F. C.; Spanggaard, H.; Rozlosnik, N.; Larsen, N. B.; Jorgensen, M. *Langmuir* **2003**, *19* (19), 7873−7880.
(17) Krebs, F. C. *Sol. Energy Mater. Sol. Cells* **2003**, *80* (2), 257−264.

10.1021/cm0528734 CCC: $33.50
Published on Web 08/10/2006

all lack the flexibility to accommodate, on a single template, molecules with varying chromophore number, spacing, and orientation. The importance of such control in biological systems is well-documented; for example, the crystal structure of the natural photosynthetic apparatus, containing the protein−cofactor complexes photosystems I and II (PSI and PSII), reveals that the light-harvesting pigments are spaced at specific distances to optimize electron coupling, photon capture, and energy transfer.[18−20] Therefore, multiple investigations aimed at integrating biological and optically active molecules have been previously reported, such as the combination of functional molecules with biologically inspired templates based on nucleic acids and peptide nucleic acids. For example, Berg et al. reported the use of diamino acid-N^{α}-substituted oligopeptides (DNOs) to force orientational order on azobenzene side chains to improve their optical properties for applications in holographic data storage,[21] although these studies did not attempt to control precise spacing of chromophores at varied distances. Later investigations of excimer formation between pyrene molecules on the DNO backbone demonstrated variations in excimer formation with changes in the length of the backbone between the pyrenes, which suggested that the short DNOs can adopt a helical structure.[22] B-DNA has also been used as a scaffold to control electronic interactions between two aligned stilbenedicarboxamide molecules at specific distances.[23] However, the chemical versatility of these approaches may be more limited than those employing peptide-based coupling strategies.

Peptides functionalized with electroactive moieties have also been shown to have interesting properties. For example, porphyrin-functionalized peptide scaffolds have been produced to mimic the photosynthetic light-harvesting complex and to study long-range electron coupling between the porphyrin molecules.[24] Alternatively, anionic porphyrin molecules have been used to induce coiled-coil structure in designed peptides, resulting in a porphyrin−peptide pair capable of electron or excitation energy transfer.[25] In another paper, porphyrin-functionalized peptide oligomers complexed with fullerene clusters have been shown to enhance the light−energy conversion efficiency in photovoltaics.[26] However, these reported peptidic systems generally lack precise placement of the chromophores (i.e., they are randomly attached to the template), and in many cases, the peptidic species alone aggregates, complicating analysis of the behavior of the isolated assemblies of chromophores. Proteins and polypeptides functionalized with chromophores in specific positions, however, have been used to study the structure, dynamics, and proximity relationships in biomolecules via fluorescence resonance energy transfer (FRET),[27,28] and in such studies helical peptides exhibiting intramolecular FRET have been reported.[29] These studies, therefore, also suggest the relevance of using peptidic templates to display electroactive groups in a well-controlled manner that may define electronic behavior. The use of peptidic structures over the nucleic acid-based approaches may offer improved chemical versatility, the ability to control the alignment of two or more chromophores, and the ability to directly couple these interactions with biologically relevant processes.

We have therefore taken advantage of the well-known capability of controlling side chain placement in peptidic α-helices to exert spatial control over the placement of conjugated side chains and to produce molecules that may be useful in the design of functional molecules for optoelectronic applications. In the long term, this design strategy will also facilitate the creation of a parallel or antiparallel assembly of multiple chromophores, structurally similar or variant, on a single molecule with accurately defined spacing. In our initial investigations, an alanine-rich, α-aminoisobutyric acid (Aib)-stabilized α-helical peptide was used as a template and was decorated with methylstilbene molecules with tunable relative spacing and orientation. The methylstilbene moieties were easily attached to the peptide via Heck coupling reactions between methylstyrene and the nonnatural amino acid *p*-bromophenylalanine (*p*-BrF), which was included in desired positions in the peptide sequence. The structures of the polar hybrid molecules were easily verified via electrospray ionization mass spectrometry (ESI-MS). The versatility of solid-phase peptide synthesis facilitates the production of various peptide templates carrying nonnatural amino acids, and the single-step chemical transformation that permits attachment of varying electroactive side chains makes this design straightforward and synthetically attractive. Furthermore, significant differences in the electronic behavior of the electroactive side chains, based on their relative positions on the peptide, can be easily monitored. This integrated approach should therefore be highly useful for determining the appropriate chemical structure and spatial orientation of organic semiconducting molecules for a variety of different and specific applications. For example, similar peptide templates could be utilized to incorporate chromophores with noncentrosymmetric molecular alignment to achieve devices for nonlinear optics application.[30] In more basic investigations, the theories of Forster energy transfer and Marcus photoinduced charge transfer could also be tested by systematically varying the energy levels, spacing, and orientation of chromophores.

(18) Barber, J. *Curr. Opin. Struct. Biol.* **2002**, *12* (4), 523−30.
(19) Saenger, W.; Jordan, P.; Krauss, N. *Curr. Opin. Struct. Biol.* **2002**, *12* (2), 244−254.
(20) McDermott, G.; Prince, S. M.; Freer, A. A.; Hawthornthwaite-Lawless, A. M.; Papiz, M. Z.; Cogdell, R. J.; Isaacs, N. W. *Nature (London)* **1995**, *374* (6522), 517−21.
(21) Berg, R. H.; Hvilsted, S.; Ramanujam, P. S. *Nature* **1996**, *383* (6600), 505−508.
(22) Reynisson, J.; Vejby-Christensen, L.; Wilbrandt, R.; Harrit, N.; Berg, R. H. *J. Pept. Sci.* **2000**, *6* (12), 603−611.
(23) Lewis, F. D.; Zhang, L.; Liu, X.; Zuo, X.; Tiede, D. M.; Long, H.; Schatz, G. C. *J. Am. Chem. Soc.* **2005**, *127* (41), 14445−14453.
(24) Dunetz, J. R.; Sandstrom, C.; Young, E. R.; Baker, P.; Van Name, S. A.; Cathopolous, T.; Fairman, R.; De Paula, J. C.; Kerfeldt, K. S. *Org. Lett.* **2005**, *7* (13), 2559−2561.
(25) Kovaric, B. C.; Kokona, B.; Schwab, A. D.; Twomey, M. A.; dePaula, J. C.; Fairman, R. *J. Am. Chem. Soc.* **2006**, *128* (13), 4166−4167.
(26) Hasobe, T.; Kamat, P. V.; Troiani, V.; Solladie, N.; Ahn, T. K.; Kim, S. K.; Kim, D.; Kongkanand, A.; Kuwabata, S.; Fukuzumi, S. *J. Phys. Chem. B* **2005**, *109* (1), 19−23.
(27) Stryer, L. *Annu. Rev. Biochem.* **1978**, *47* (1), 819−846.
(28) Wu, P. G.; Brand, L. *Anal. Biochem.* **1994**, *218* (1), 1.
(29) Hossain, M. A.; Mihara, H.; Ueno, A. *J. Am. Chem. Soc.* **2003**, *125* (37), 11178−11179.
(30) Kauranen, M.; Verbiest, T.; Boutton, C.; Teerenstra, M. N.; Clays, K.; Schouten, A. J.; Nolte, R. J. M.; Persoons, A. *Science (Washington, D. C.)* **1995**, *270* (5238), 966−9.

Table 1. Peptide Sequences

peptide sequence	name	position	D^a (Å)
Ac-KAA-Aib-KAA-Aib-A**X**A-Aib-AA**X**-Aib-AAK-Aib-AAKGG Y-NH_2	7 offset (**7O**)	$i, i+5$	7
Ac-KA-Aib-AKA-Aib-A**X**A-Aib-AAA-Aib-**X**AA-Aib-KAAKGG Y-NH_2	11 dimer (**11D**)	$i, i+7$	11
Ac-KAA-Aib-KAA-Aib-A**X**A-Aib-A**X**A-Aib-AAK-Aib-AAKGGY-NH_2	6 dimer (**6D**)	$i, i+4$	6
Ac-KA-Aib-AKA-Aib-A**X**AA**X**A-Aib-A**X**A-Aib-AKA-Aib-AKGGY-NH_2	6 trimer (**6T**)	$i, i+3$; $i, i+4$	6

[a] Approximate distance between the two residues on the peptide backbone denoted by **X** in the sequence above, as determined from energy-minimized structures generated with the Insight II suite of molecular modeling software. **X** in the peptide sequence (Table 1) may represent either *p*-BrPhe or (*p*-methylstyryl)phenylalanine. The **6D** peptide containing *p*-BrPhe will be represented throughout the text as **BrF-6D** and the peptide with the methylstilbene side chain as **S-6D**; similar notation will be used to represent the other peptides.

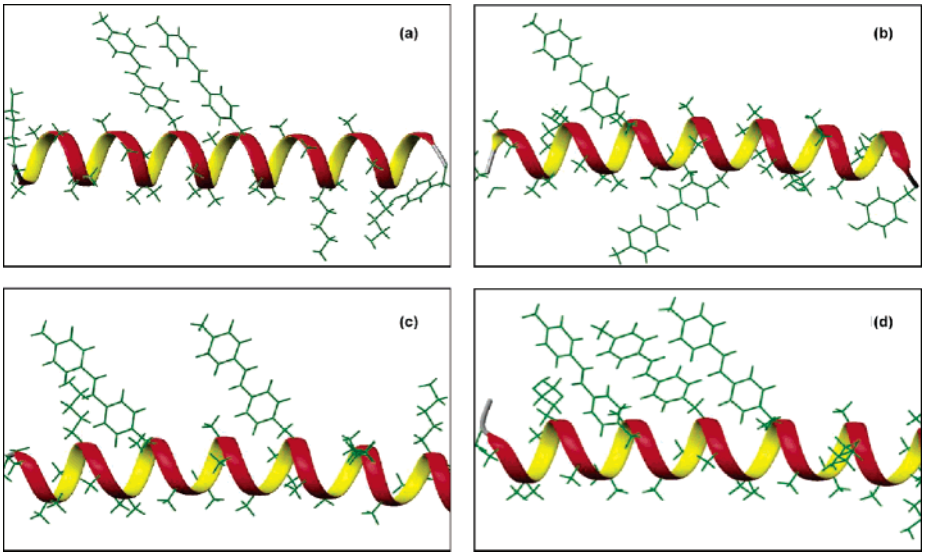

Figure 1. Representative schematics of energy-minimized structures of peptides equipped with methylstilbene side chains, indicating their probable arrangement: (a) **S-6D**; (b) **S-7O**; (c) **S-11D**; (d) **S-6T**. These figures were created using the Insight II suite of software and rendered using MOLMOL.

Results and Discussion

CD Behavior. The specific peptide sequences employed in these investigations are shown in Table 1. All of the peptides are based on an AAA**X** repeating sequence, in which the high helical propensity of alanine confers a strong tendency for α-helix formation.[31] Aib residues were introduced throughout the peptide to increase the thermal stability of the helix[32] and to minimize possible distortions in the helical conformation after grafting of bulky side groups onto the peptide backbone. Lysine was included in the sequences to prevent peptide aggregation in solution; indeed, the parent and modified peptides of Table 1 were revealed on the basis of CD investigations to be monomeric in aqueous solution (see below).[33] Tyrosine was placed at the C-terminus of the helix for concentration determination purposes. The use of these peptidic molecules permits positioning of the reactive groups, denoted by **X** in Table 1, either on the same side of the helical backbone or on the opposite side, with a well-defined intermolecular distance. Energy-minimized structures of the chemically modified peptides (Figure 1), which illustrate the positioning of the conjugated side chains, were used to estimate these distances. The helicity of the peptides as a function of increasing temperature was determined via circular dichroic (CD) spectroscopic analysis of the peptides in trifluoroethanol (TFE) (Figure 2a). All the peptides displayed a characteristic α-helical spectrum with double minima at 208 and 222 nm and a single maximum at 192 nm (Figure 2a). The concentration dependence of the mean residue ellipticity θ_{MRE} and the thermally induced transition between helix and random coil, between 100 nM and 100 μM, was investigated for the most hydrophobic peptide, **S-6T** (data not shown). θ_{MRE} (at 25°C) and the melting curves were identical over this concentration range, indicating that the chemically modified peptides are monomeric. Additionally, **S-6D**, **S-7O**, and **S-11D** have equivalent θ_{MRE} values at 25°C; thus, the impact of methylstilbene placement on PL can be directly compared. **S-6T** is also similarly helical at 25 °C, with θ_{MRE} values only slightly lower than those of the other chemically modified peptides. Thermal unfolding experiments were performed on all the peptides listed in Table 1 to estimate the folded fraction of each peptide as a function of temperature. The results are shown in Figure 2b and demonstrate that all of these helical peptides are stable, showing an incomplete conversion between helical and a nonhelical conformation and retaining at least 40% of their original helicity even at elevated temperatures (80 °C). The similarity in the helicity and temperature-dependent conformational behavior of the modified and unmodified peptides indicates that the bulkier conjugated side groups on the chemically modified peptide do not substantially influence the helical content or thermal stability, suggesting the broad utility of such templates for displaying various kinds of conjugated side chains.

(31) Chakrabartty, A.; Kortemme, T.; Baldwin, R. L. *Protein Sci.* **1994**, *3* (5), 843−852.
(32) De Filippis, V.; De Antoni, F.; Frigo, M.; de Laureto, P. P.; Fontana, A. *Biochemistry* **1998**, *37* (6), 1686−1696.
(33) Padmanabhan, S.; Marqusee, S.; Ridgeway, T.; Laue, T. M.; Baldwin, R. L. *Nature* **1990**, *344* (6263), 268−270.

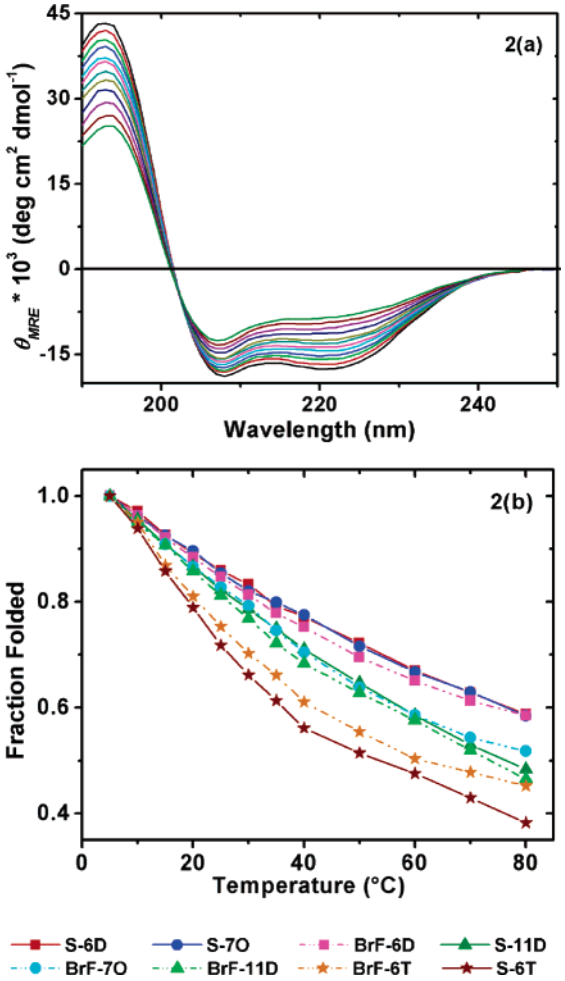

Figure 2. Circular dichroic data for the peptides of Table 1: (a) CD scans reported as a function of increasing temperature (5−80 °C) for the **S-6D** peptide in TFE; (b) thermal unfolding scans of peptides in TFE.

PL Behavior. The impact of the varied relative positioning of the conjugated side chains on their electronic behavior was assessed via PL experiments on the methylstilbene-modified peptides in TFE[34] (Figure 3). While all four peptides (**S-6D**, **S-6T**, **S-7O**, and **S-11D**) show identical absorption spectra (Figure 3a) and exhibit monomeric methylstilbene emission with a peak maximum at 357 nm (Figure 3b), they exhibit significantly different PL intensities as a function of peptide architecture (Figure 3b). In particular, **S-7O** and **S-11D** show only excitonic monomer emission with peak intensities and, therefore, fluorescence quantum yields that are identical. Given that the methylstilbene side chains in **S-7O** are placed on opposite sides of the helix, and that the CD data indicate that the peptides do not interact in solution at these low peptide concentrations, it can be assumed that **S-7O** is representative of an isolated molecule system with pure molecular stilbene excitons. The identical PL spectra for **S-7O** and **S-11D** indicate that the methylstilbene molecules do not interact with each other when displayed on the **S-11D** peptide and, therefore, the PL is purely excitonic in origin when the electroactive groups are separated by a

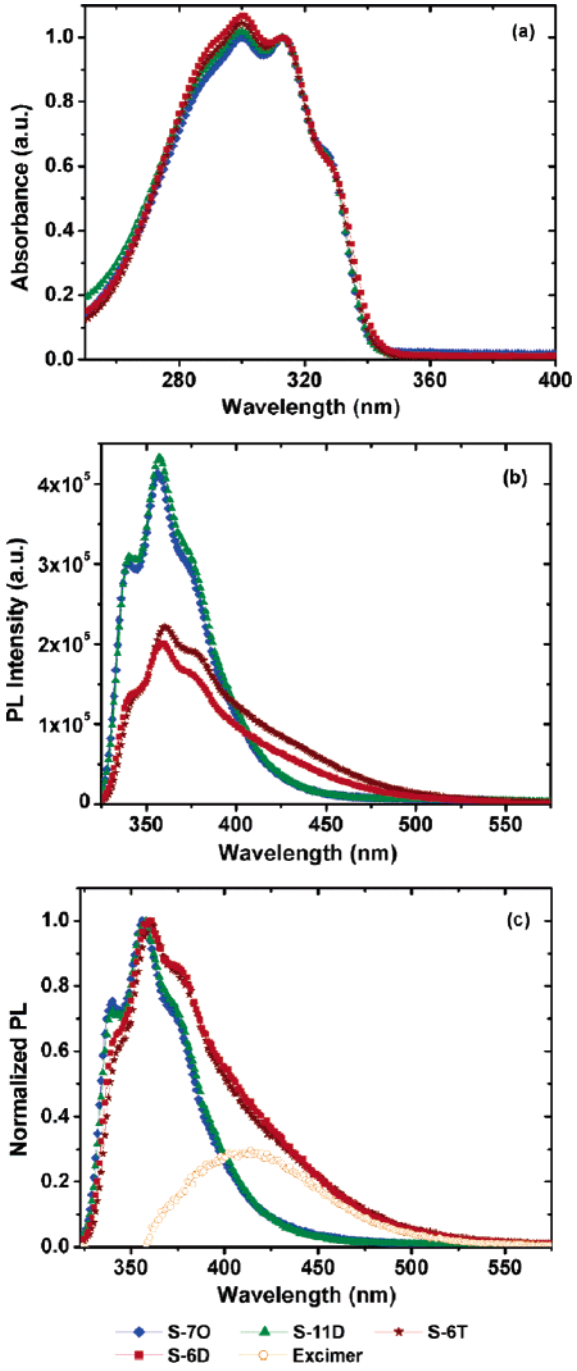

Figure 3. Absorption and photoluminescence spectra: (a) absorption spectra normalized to the intensity at 313 nm; (b) PL spectra after excitation at 313 nm; (c) PL spectra normalized to the maximum intensity at 357 nm.

distance of 11 Å. Indeed, these results are consistent with theoretical predictions.[35] In contrast, **S-6D** and **S-6T** are shown to exhibit a greater than 50% reduction in PL intensity, with a transition evident in the low-energy region of the **S-6D** and **S-6T** PL spectra, indicating the association of the methylstilbene side chains. Upon subtraction of the **S-7O** spectrum from either the normalized **S-6D** or **S-6T** spectrum, the low-energy transition is revealed as shown in Figure 3c. This broad, featureless, red-shifted, and low-quantum-yield fluorescence is due to formation of an excimer and not from any ground-state association, as no corresponding peak is

(34) We observed that tyrosine and the amide bonds do not have any contribution to PL when excited at 313 nm (absorption maximum of the stilbene molecules), which implies that the photophysics of the electroactive arms can be monitored by PL without any peptide template interference.

(35) Cornil, J.; dos Santos, D. A.; Crispin, X.; Silbey, R.; Bredas, J. L. *J. Am. Chem. Soc.* **1998**, *120* (6), 1289−1299.

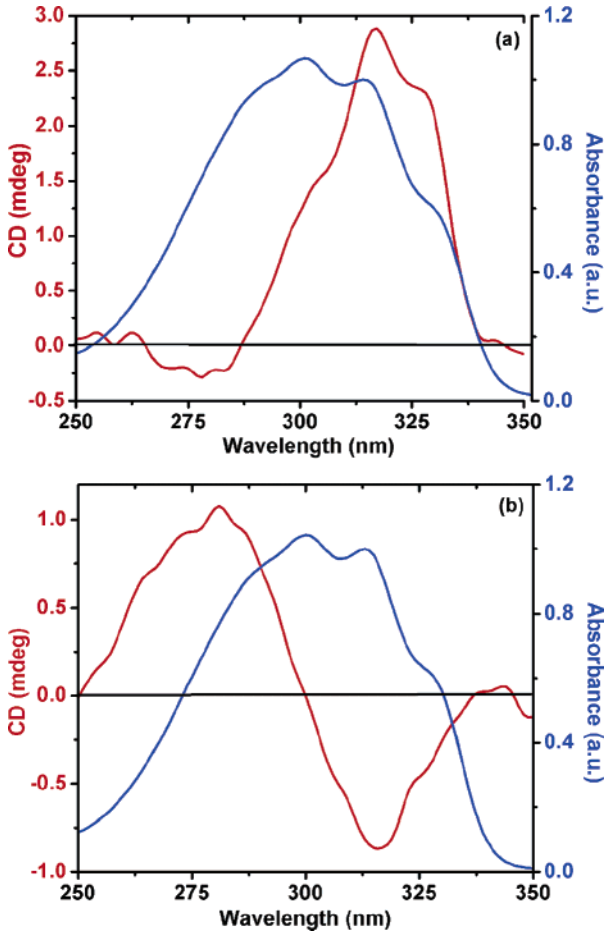

Figure 4. Exciton-coupled CD spectra for **S-6D** (a) and **S-6T** (b). The red spectrum shows the CD, while the blue spectrum indicates the absorption band of the transition. The split Cotton effect for both **S-6D** and **S-6T** is a result of the close proximity and chiral orientation of the chromophores.

observed in the absorption spectra (Figure 3a).[36,37] Furthermore, the excimer emission shown in Figure 3c is similar to the reported emission from excited-state dimers of stilbene derivatives,[38] which suggests that the methylstilbene side chains in **S-6D** and **S-6T** form excimers even at very dilute concentrations as a result of their controlled proximity mediated by the helical peptide. The exciton emission (monomer emission) in the PL spectra of **S-6D** and **S-6T** may appear because the peptides are not fully helical at room temperature as indicated via CD.

Exciton-Coupled CD Behavior. Near-UV circular dichroism experiments were conducted to probe the relative orientation and chromophore interactions of the methylstilbene side chains on the peptide templates that demonstrated excited-state coupling between side chains, **S-6T** and **S-6D** (Figure 4). Both hybrid biomolecules showed an active response to circularly polarized light in the methylstilbene absorption envelope; no such response was observed for unmodified peptide or neat stilbene. A split Cotton effect was observed for both **S-6D** and **S-6T**, although the signs of the split were different (parts a and b, respectively, of Figure 4). These results indicate that the methylstilbene side chains have a chiral orientation with respect to one another, and are able to undergo exciton coupling owing to their close proximity.[39,40] The opposite signs of the split peaks of **S-6D** and **S-6T** may suggest a difference in the relative orientations or the screw sense of the methylstilbene molecules. **S-6T** shows a conventional split Cotton effect behavior; the asymmetric split observed for **S-6D** may be a result of coupling with other electronic transitions or of additional background ellipticity, as has been observed in other previously reported systems.[39,41] It may also arise from the difference in the number of chromophores on the peptides or from small differences in the folding of the helical templates. Nevertheless, these CD results confirm the proximity of the conjugated side chains on the peptidic backbone at distances that permit exciton coupling, despite slight differences in the chirality of the side chain orientation.

Photoluminescence Excitation (PLE) Behavior. PLE spectroscopy experiments were conducted to highlight changes in ground-state interactions that might occur as a function of side chain placement; the data are summarized in Figure 5. The PLE data were collected at 450 nm after excitation over the full spectrum, since monomer emission from **S-7O** and **S-11D** was observed to be negligible at 450 nm (Figure 4b). The appearance of a new peak at 371 nm for **S-6D** (Figure 5a) demonstrates that **S-6D** forms very strong intermolecular ground-state interactions in addition to its interactions in the excited state (excimer formation); the peptide backbone must therefore hold the methylstilbene molecules in close proximity and permit ground-state interactions. Similar observations of associated electroactive species via PLE experiments with excitation to the red edge of the excitonic absorption have been previously reported,[42−44] suggesting the viability of this interpretation. Although this new state is not detected via absorption spectroscopy, it may be evident in the PLE spectra because PL is far more sensitive and aggregate selective than absorption spectroscopy.[45] In addition, of all the peptides, only **S-6D** shows detectable PL after excitation at the absorption maximum of the ground-state complex, i.e., 371 nm (Figure 5b), suggesting that the ground-state complex must have a high PL quantum yield despite its very low extinction coefficient in the absorption spectrum. Similar findings have been reported for poly(*p*-pyridylvinylene) (PPyV) systems[44] and for poly(9,9-dioctylfluorene),[43] in which a distinct signature

(36) Pope, M.; Swenberg, C. E. *Electronic Processes in Organic Crystals and Polymers*, 2nd ed.; Oxford University Press: New York, 1999.
(37) Samuel, I. D. W.; Rumbles, G.; Collison, C. J. *Phys. Rev. B* **1995**, *52* (16), 11573−11576.
(38) Wang, S. J.; Bazan, G. C. *Chem. Phys. Lett.* **2001**, *333* (6), 437−443.
(39) Harda, N.; Nakanishi, K. *Circular Dichroic Spectroscopy-Exciton Coupling in Organic Stereochemistry*; University Science Books: Mill Valley, CA, 1983.
(40) Nakanishi, K.; Berova, N. Exciton Chirality Method: Principles and Applications. In *Circular Dichroism, Principles and Applications*, 2nd ed.; Nakanishi, K., Berova, N., Woody, R., Eds.; VCH Publishers: New York, 1994; pp 337−395.
(41) Matile, S.; Berova, N.; Nakanishi, K.; Fleischhauer, J.; Woody, R. W. *J. Am. Chem. Soc.* **1996**, *118* (22), 5198−5206.
(42) Nguyen, T. Q.; Doan, V.; Schwartz, B. J. *J. Chem. Phys.* **1999**, *110* (8), 4068−4078.
(43) Grell, M.; Bradley, D. D. C.; Long, X.; Chamberlain, T.; Inbasekaran, M.; Woo, E. P.; Soliman, M. *Acta Polym.* **1998**, *49* (8), 439−444.
(44) Blatchford, J. W.; Gustafson, T. L.; Epstein, A. J.; VandenBout, D. A.; Kerimo, J.; Higgins, D. A.; Barbara, P. F.; Fu, D. K.; Swager, T. M.; MacDiarmid, A. G. *Phys. Rev. B* **1996**, *54* (6), R3683−R3686.
(45) Turro, N. J., *Modern Molecular Photochemistry*; University Science Books: Sausalito, CA, 1991.

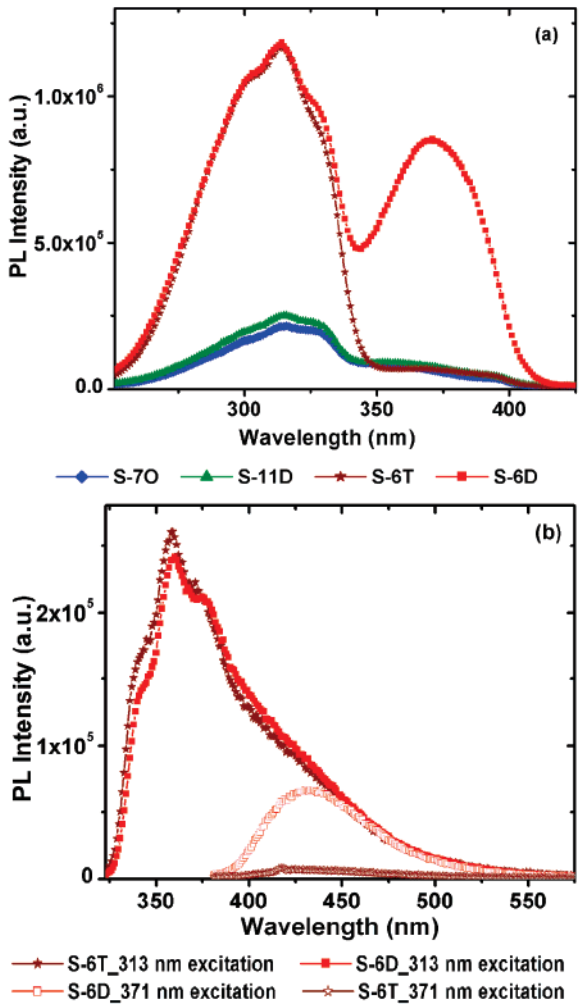

Figure 5. PLE spectra of the peptides (a) and ground-state complex (b). The detection wavelength was set to 450 nm, where a high excimer to monomer PL ratio is observed.

peak at the red edge of the absorption spectrum and a greater emission for the aggregates versus excimers were observed. Furthermore, while the intrinsic PL quantum yield for stilbene molecules is reported to be 5% in nonviscous organic solution,[46−49] this efficiency increases up to 75% in rigid environments that prevent the torsional angle twist at the vinyl bonds that break the conjugation.[45] This set of previous observations substantiates that the interaction of methylstilbene moieties in **S-6D** results in a rigid complex with restricted torsional angles at the vinyl bond and a corresponding high PL quantum yield upon excitation at 371 nm. In fact, analogous spectral assignments have been previously reported for a methylstilbene dimer with brick-wall geometry.[50] The observed excimer formation but lack of ground-state interactions for **S-6T** suggests that slight differences in side chain placement, as also predicted from the exciton-coupled CD data, prevent the formation of a similar rigid complex in the ground state (see below).

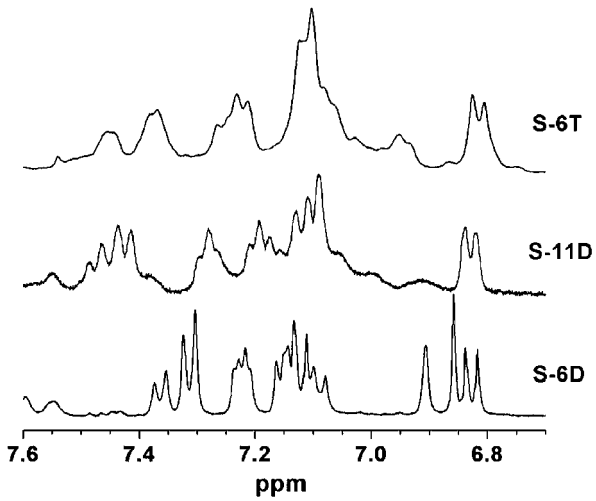

Figure 6. NMR spectra of **S-6D**, **S-6T**, and **S-11D**. Samples of 1 mg/mL concentration were prepared in 90:10 *d*-TFE/D_2O solution and scanned overnight. Concentrations were minimized to avoid intermolecular interactions between peptide templates.

^{1}H NMR Behavior. ^{1}H NMR experiments were also performed to explore the extent of ground-state aromatic interactions between the methylstilbene molecules on peptides designed to present the conjugated side chains on the same face of the helix. ^{1}H NMR experiments were performed on **S-6D**, **S-11D**, and **S-6T** at concentrations of 1 mg/mL in 90/10 *d*-TFE/D_2O; the resulting data are shown in Figure 6. The aromatic resonances of tyrosine, δ (ppm) 6.80−6.85, essentially overlap for all three peptides, permitting direct comparison of the chemical shifts of other resonances in this region. The breadth of the resonances of **S-6T** almost certainly arises from peptide aggregation at the concentrations necessary for the NMR experiments; no such aggregation was indicated in the lower concentrations, 0.05−0.2 mg/mL, employed in the PL and CD experiments. Similarly, the slight broadening of the resonances of **S-11D** may also arise from a small extent of peptide aggregation, while the sharp resonances for **S-6D** suggest that there is no aggregation of this peptide under these experimental conditions. As shown in Figure 5, an upfield shift greater than 0.1 ppm in the aromatic peaks, δ (ppm) 7.0−7.5, and a 0.23 ppm shift in the vinyl peaks, δ (ppm) 7.09−7.12, are observed upon comparison of **S-6D** and **S-11D**; such upfield shifts in the range of 0.1−0.5 ppm are well-documented as an indication of $\pi-\pi$ stacking.[13,51−54] The sharpness of the **S-6D** resonances, coupled with their significant upfield shift relative to the resonances in both **S-11D** and **S-6T**, is a clear indication that the conjugated side chains of **S-6D** are aligned as a result of their presentation on the helical peptide, and not due to the interaction of side chains on different peptides, which was also indicated by CD experiments. These observed shifts also corroborate the PL and PLE results, indicating a ground-state interaction of the methylstilbene side chains in

(46) Waldeck, D. H. *Chem. Rev.* **1991**, *91* (3), 415−436.
(47) Samsonova, L. G.; Kopylova, T. N.; Svetlichnaya, N. N.; Andrienko, O. S. *High Energy Chem.* **2002**, *36* (4), 276−279.
(48) Malkin, S.; Fischer, E. *J. Phys. Chem.* **1962**, *66* (12), 2482.
(49) Malkin, S.; Fischer, E. *J. Phys. Chem.* **1964**, *68* (5), 1153.
(50) Ruseckas, A.; Namdas, E. B.; Lee, J. Y.; Mukamel, S.; Wang, S. J.; Bazan, G. C.; Sundstrom, V. *J. Phys. Chem. A* **2003**, *107* (40), 8029−8034.
(51) Niazimbetova, Z. I.; Christian, H. Y.; Bhandari, Y. J.; Beyer, F. L.; Galvin, M. E. *J. Phys. Chem. B* **2004**, *108* (25), 8673−8681.
(52) Colquhoun, H. M.; Zhu, Z. X.; Cardin, C. J.; Gan, Y. *Chem. Commun.* **2004** (23), 2650−2652.
(53) Viel, S.; Mannina, L.; Segre, A. *Tetrahedron Lett.* **2002**, *43* (14), 2515−2519.
(54) Solladie, N.; Walther, M. E.; Gross, M.; Duarte, T. M. F.; Bourgogne, C.; Nierengarten, J. F. *Chem. Commun.* **2003** (19), 2412−2413.

S-6D via $\pi-\pi$ stacking. The degree of interaction between the methylstilbene groups on **S-6T** cannot be clearly ascertained from these experiments, owing to the peak broadening; the slight upfield shift observed for the resonances likely results at least in part from peptide aggregation rather than side chain association.

The combination of the exciton-coupled CD, PL, PLE, and NMR results clearly demonstrates that the interaction of conjugated side chains can be precisely prescribed via presentation of these side chains on an appropriate peptide template. Such presentation mediates almost face-to-face packing of the methylstilbene side chains in **S-6D** as suggested by the PLE and NMR data, although this cofacial dimerization appears to be significantly reduced in the case of **S-6T**, perhaps because **S-6T** is slightly less helical than **S-6D** (Figure 2b). Taken altogether, these results reveal slight structural differences between the peptides that affect nuances of their electronic behavior, explain the formation of the ground state in **S-6D**, and indicate the ability to control the placement of multiple electroactive species on peptidic templates. They also suggest important opportunities for studying and designing additional electroactive molecules of new compositions for device applications.

Conclusion

A novel α-helical peptide hybrid has been shown to be useful for the alignment of multiple electroactive molecules with precisely controlled intermolecular spacing and orientations. Detailed characterization of the hybrid peptides via multiple methods indicates that π orbital interactions at the molecular level are very sensitive to the intermolecular distances and orientations that are accessible via the use of a peptide template. Interactions are present when molecules are cofacial and near 6 Å apart, but the extent and type of interaction depend on slight variations in side chain presentation. Interactions are absent after an increase in the intermolecular separation to around 11 Å or upon an offset from the cofacial state. This use of a peptide template permits investigation of filmlike aggregation behavior of organic electroactive molecules, yet in dilute solution, with the potential for remarkable control over the number of molecules in the aggregate. Although initial systems have employed methylstilbene as the electroactive species, the organization of varied electron- and hole-transporting groups with longer conjugation lengths is also under investigation. Given the exceptionally versatile nature of the chemical modification strategies, these templates may also be employed to organize chemically different electroactive oligomers to form heterodimers and to explore distance and orientation dependence in other phenomena such as energy transfer and exciton splitting.

Experimental Section

Peptide Synthesis and Characterization. Peptides were synthesized on a Rink amide MBHA resin (Novabiochem, San Diego, CA) using automated solid-phase peptide synthesis methods (PS3, Protein Technologies, Inc., Tucson, AZ). The amino acid residues were activated for coupling with HBTU in the presence of 0.4 M methylmorpholine in DMF. Deprotections were carried out in 20% piperidine in DMF for approximately 10 min. Standard coupling cycles were used for the first 10 couplings (60 min), and extended coupling cycles (2 h) were used to complete the sequence. The N-terminus was acetylated with 5% acetic anhydride in DMF for 30 min. Cleavage of the peptide from the resin was performed in 95:2.5:2.5 trifluoroacetic acid (TFA)/triisopropylsilane (TIPS)/water for 3−4 h. TFA was evaporated, and the cleavage products were dissolved in ether. The water-soluble peptides were extracted with water and lyophilized. Peptides were purified via reversed-phase HPLC (Waters, MA), using a Symmetry C-18 column. The identity of each peptide was confirmed via ESI-MS (AutospecQ, VG Analytical, Manchester, U.K.): (**BrF-6D**) *m*/*z* 2578.5 (M^+), calcd 2578.75; (**BrF-7O**) *m*/*z* 2578.5 (M^+), calcd 2578.75; (**BrF-11D**) *m*/*z* 2578.5 (M^+), calcd 2578.75; (**BrF-6T**) *m*/*z* 2805.6 (M^+), calcd 2806.

General Procedure for Functionalizing the Peptides. *p*-Methylstyrene was separated from inhibitors via distillation over CaH_2. Heck coupling between *p*-methylstyrene and peptide was carried out under a dry nitrogen atmosphere with anhydrous DMF. First, a solution of 25 mmol of *p*-methylstyrene and 20 mmol of tributylamine was prepared in 2 mL of DMF. This solution was added to a 10 mmol peptide template (for a peptide with two Br functionalities), 4 mmol of tri-*o*-tolylphosphine, and 0.8 mmol of palladium(II) acetate mixture in the reaction flask. The reaction was kept at 70 °C in an oil bath. The progress of the reaction was monitored via ESI-MS, and when necessary, initial amounts of the reactant, ligand, and catalyst were added again. The final reaction mixture was precipitated in ether to extract the water-soluble peptide. Excess ether was removed via freeze-drying, and the modified peptides were purified via reversed-phase HPLC as above. The identity of each peptide was confirmed via ESI-MS: (**S-6D**) *m*/*z* 2654.7 (M^+), calcd 2654.9; (**S-7O**) *m*/*z* 2654.7 (M^+), calcd 2654.9; (**S-11D**) *m*/*z* 2654.7 (M^+), calcd 2654.9; (**S-6T**) *m*/*z* 2917.8 (M^+), calcd 2918.2.

Characterization of the Hybrid Molecules. Molecular modeling was performed on the peptides using Insight II molecular modeling software (Accelrys Software Inc., San Diego, CA). Energy minimization studies were done using cff91 force fields in TFE, setting the dielectric constant of the medium to 26.5, and using 30000 conjugate gradient iterations. Circular dichroic spectra were recorded on a Jasco-810 spectropolarimeter (Jasco, Inc., Easton, MD) using a 0.1 cm path length cell and a scan rate of 50 nm/min. The spectra reported are averages of three scans with a standard deviation of 3%. CD spectra were recorded for each peptide as a function of increasing temperature from 190 to 250 nm to determine the helicity, and CD spectra in the near-UV (250−400 nm) were also collected to investigate the CD of the methylstilbene side chain. The concentration of the *p*-BrPhe-containing peptides was calculated by using the extinction coefficient of the tyrosine residue at 374 nm ($\epsilon = 1404\ M^{-1}\ cm^{-1}$), and the concentration of methylstilbene peptides was measured using amino acid analysis. Data points for the wavelength-dependent CD spectra were recorded every 1 nm with a 1 nm bandwidth. Data points for the temperature scans were recorded at 222 nm, at 1 °C intervals with an equilibration time of 1 min. The mean residue ellipticity, θ_{MRE}, (deg cm^2 $dmol^{-1}$) was calculated via use of the molecular weight of the peptide and cell path length. In prior experiments done on *p*-bromophenylalanine, *trans* isomer formation upon Heck reaction was confirmed via the presence of the *trans*-vinyl bending peak (964 cm^{-1}) and the absence of the *cis*-vinyl bending peak in FTIR (Fourier transform infrared) spectra. NMR spectra were obtained at room temperature via the use of a Bruker DRX 400 MHz spectrometer. A 1 mg/mL solution of the peptide in *d*-TFE/D_2O (90:10) was analyzed overnight. UV−vis absorption spectra were measured on an Agilent 8453 spectrophotometer. PL and PLE experiments were performed

on a SPEX Fluoromax 3 spectrofluorimeter using Datamax software. All the photophysical experiments were performed on dilute solutions of peptides with a methylstilbene absorption maximum of ~0.1.

Acknowledgment. This work was funded in part by grants from the National Science Foundation (DMR 0210223 and DMR 0239744) and the National Institutes of Health (5 P20 RR15588). We thank Lewis Rothberg (University of Rochester), Nina Berova (Columbia University), and Joseph Fox (University of Delaware) for helpful and insightful discussions.

CM0528734